

Holographic thermalization in noncommutative geometry

Xiao-Xiong Zeng ^{1*}, Xian-Ming Liu ^{2†}, Wen-Biao Liu (corresponding author) ^{3‡}

¹*School of Science, Chongqing Jiaotong University, Chongqing, 400074, China*

²*Department of Physics, Hubei University for Nationalities, Enshi, 445000, Hubei, China*

³*Department of Physics, Institute of Theoretical Physics, Beijing Normal University, Beijing, 100875, China*

Abstract

Gravitational collapse of a shell of dust in noncommutative geometry is probed by the renormalized geodesic length, which is dual to probe the thermalization by the two-point correlation function in the dual conformal field theory. We find that larger the noncommutative parameter is, longer the thermalization time is, which implies that the large noncommutative parameter delays the thermalization process. We also investigate how the noncommutative parameter affects the thermalization velocity and thermalization acceleration.

1. Introduction

Gravity in noncommutative geometry[1, 2] and noncommutative field theory [3, 4] has been investigated extensively in recent years. The reason for this prevailing phenomenon maybe arises from a fact that the singularities in general relativity and ultraviolet divergences in quantum field theory can be avoided in the noncommutative framework. Because in noncommutative geometry, coordinates in a manifold fail to commute in analogy to the conventional noncommutativity among conjugate variables in quantum mechanics, which leads to a natural cut off due to the position uncertainty.

To study the properties of gravity in the noncommutative geometry, it is important and necessary to find the black hole solutions in this background.

*E-mail address: xxzengphysics@163.com

†E-mail address: liuxianming1980@163.com

‡E-mail address: wblu@bnu.edu.cn

Because spacetime as a manifold of points breaks down at distance scale of the order of the Planck length, it was proposed that the point-like object should be replaced by a smeared object[5, 6]. In this case, the description mathematically by a Dirac-delta function distribution is substituted by a Gaussian distribution of minimal width $\sqrt{\theta}$, where θ is the smallest fundamental unit of an observable area in the noncommutative coordinates. The first noncommutative black hole solution was presented by Nicolini, Smailagic and Spallucci using the coordinate coherent state method[7]. It was found that the curvature singularity of the black hole is removed. Moreover, their method is consistent with Lorentz invariance, unitarity and UV finiteness of quantum field theory, which appears in the Weyl-Wigner-Moyal \star -product approach. Until now, there are many investigations on the properties of the noncommutative black hole, such as thermodynamic properties[8], quantized entropy and area of horizon[9], quantum tunneling radiation[10], gravitational collapse solution[11], strong gravitational lensing effect[12], and so on. Especially recently, Hawking-Page phase transition[13], holographic entanglement entropy[14], and holographic superconductors[15] have also been investigated as the noncommutative anti-de Sitter black hole solution[16] is given.

In this paper, we intend to investigate the non-equilibrium thermalization process in noncommutative field theory from the viewpoint of holography. Recent years, investigation on holographic thermalization has attracted more and more attentions of theoretical physicist. The main motivation maybe arises from a fact that the thermalization time of quark gluon plasma produced in RHIC and LHC experiments predicted by the perturbation theory is longer than the experiment result [17]. In order to investigate the thermalization process, one should construct a proper model in gravity [18]. Now, there have been many models to study the non-equilibrium thermalization process [19, 20, 21, 22, 23, 24, 25, 26, 27, 28, 29, 30, 31]. Among them, one elegant model is presented in [30, 31], where the two-point correlation function, Wilson loop, and entanglement entropy were used to detect the thermalization. Now, such an investigation has been generalized to many gravity models [32, 33, 34, 35, 36, 37, 38, 39, 40, 41, 42, 43, 44, 45, 46, 47, 48, 49].

The purpose of this paper is to investigate how the noncommutative parameter affects the thermalization process. In the dual conformal field theory, we take the two-point correlation function as a thermalization probe

⁴ to study the thermalization behavior. According to the AdS/CFT correspondence, this process equals to probing the evolution of a shell that interpolates between a pure AdS and a noncommutative AdS black brane by the geodesic. Concretely we first study the motion profile of the geodesic, and then the renormalized geodesic length. For the spacetime with a horizon, we find for both the thermalization probes, larger the noncommutative parameter is, longer the thermalization time is. For the spacetime without a horizon, we find the shell will not collapse all the time but will stop in a stable state. In addition, we also obtain the fitting functions of the thermalization curve for both thermalization probes. Based on the functions, we get the thermalization velocity and thermalization acceleration.

The remainder of this paper is organized as follows. In the next section, we shall provide a brief review of the gravitational collapse solution in the noncommutative geometry. Then in Section 3, the collapse of the shell is probed by making use of the renormalized geodesic length. The last section is devoted to our conclusions.

2. The noncommutative Vaidya AdS black branes

In this section, we will give a brief review of the noncommutative Vaidya AdS black branes. For details, please see[16]. As well known, the metric for a static spherically symmetric noncommutative AdS black hole is[16]

$$ds^2 = -f(r)dt^2 + f^{-1}(r)dr^2 + r^2d\phi^2 + r^2\sin^2\phi d\varphi^2, \quad (1)$$

where

$$f(r) = 1 - \frac{4M\gamma(\frac{3}{2}, \frac{r^2}{4\theta})}{r\sqrt{\pi}} + \frac{r^2}{S^2}, \quad (2)$$

in which S is the radius of the AdS, M is the total mass diffused throughout the region of linear size $\sqrt{\theta}$, θ comes from the noncommutator of $[x^\mu, x^\nu] = i\theta^{\mu\nu}$ with $\theta^{\mu\nu} = \theta\text{diag}[\epsilon_1, \dots, \epsilon_{D/2}]$, and $\gamma(\frac{3}{2}, \frac{r^2}{4\theta})$ is the lower incomplete Gamma function defined by

$$\gamma(\frac{3}{2}, \frac{r^2}{4\theta}) \equiv \int_0^{\frac{r^2}{4\theta}} t^{\frac{1}{2}} e^{-t} dt. \quad (3)$$

⁴Expectation value of Wilson loop and entanglement entropy also can be treated as the thermalization probes, it has been found [30, 31] that all of them have similar behavior thus here we only use the two-point correlation.

The black hole temperature in the noncommutative geometry is given by

$$T_{NC} \equiv \frac{\kappa}{2\pi} = \frac{1}{4\pi} \frac{\partial f(r)}{\partial r} \Big|_{r_h}, \quad (4)$$

where r_h is the event horizon of the black hole determined by $f(r_h) = 0$. In addition, according to the properties of gamma function

$$\gamma(a+1, x) = a\gamma(a, x) - x^a e^{-x}, \quad (5)$$

$$\gamma\left(\frac{1}{2}, x^2\right) \equiv 2 \int_0^x e^{-t^2} dt = \sqrt{\pi} \text{Erf}(x), \quad (6)$$

Eq.(2) changes into

$$f(r) = 1 - \frac{2M}{r} \text{Erf}\left(\frac{r}{2\sqrt{\theta}}\right) + \frac{r^2}{S^2} + \frac{2M}{\sqrt{\pi\theta}} e^{-\frac{r^2}{4\theta}}, \quad (7)$$

where $\text{Erf}(\frac{r}{2\sqrt{\theta}})$ is a Gauss error function. It is obvious that this black hole spacetime is closely dependent on the noncommutative parameter θ . As $\theta \rightarrow 0$, this background reduces to the conventional Schwarzschild AdS black hole. In this case, noncommutative fluctuations are negligible and the spacetime can be well described by a classical manifold.

As done in [50], we can also consider the limit where the boundary of AdS_{d+1} is R^d instead of $R \times S^{d+1}$, namely the so-called infinite volume limit. After the coordinate transformation $z = \frac{S^2}{r}$, Eq.(1) and the components of metric in this case change into

$$ds^2 = \frac{1}{z^2} [-H(z)dt^2 + H^{-1}(z)dz^2 + dx_i^2], \quad (8)$$

$$H(z) = 1 - 2M \text{Erf}\left(\frac{1}{2\sqrt{\theta}z}\right)z^3 + \frac{2Mz^2}{\sqrt{\pi\theta}} e^{-\frac{1}{4\theta z^2}}, \quad (9)$$

where S has been set to one and $i = 1, 2$. Introducing the Eddington-Finkelstein coordinate system, namely

$$dv = dt - \frac{1}{H(z)} dz, \quad (10)$$

the background spacetime in Eq.(8) changes into

$$ds^2 = \frac{1}{z^2} [-H(z)dv^2 - 2dz dv + dx_i^2]. \quad (11)$$

Now noncommutative Vaidya AdS black brane can be obtained by freeing the mass parameter in Eq.(9) as an arbitrary function of v . As stressed in [51], in this case, the mass source includes the new matter related to the noncommutativity as well as the matter on the shell. In other words, Eq.(11) can be treated as the solution of the following field equation

$$R_{\mu\nu} - \frac{1}{2}Rg_{\mu\nu} + \Lambda g_{\mu\nu} = 8\pi G(T_{\mu\nu}^\theta + T_{\mu\nu}^m), \quad (12)$$

where $T_{\mu\nu}^\theta$ is the energy-momentum tensor arising from the noncommutative background and

$$T_{\mu\nu}^m \propto 2z^2 \frac{dM(v)}{dv} \delta_{\mu v} \delta_{\nu v}. \quad (13)$$

Here $M(v)$ is mass of a collapsing noncommutative black brane, which is usually chosen as the smooth function

$$M(v) = \frac{M}{2} \left(1 + \tanh \frac{v}{v_0} \right), \quad (14)$$

where v_0 represents a finite shell thickness. For Eq.(14), in the limit $v \rightarrow -\infty$, the mass vanishes and the background in Eq.(11) thus corresponds to a pure AdS space. In the limit $v \rightarrow \infty$, the mass changes into a constant and so the background represents a static noncommutative Schwarzschild AdS black brane.

3. Probe of the thermalization

As the model that describes the thermalization process on the dual conformal field theory is constructed, we will choose the two-point correlation function at equal time to explore how the noncommutative parameters affects the thermalization process. According to the AdS/CFT correspondence, the equal time two-point correlation function under the saddle-point approximation can be holographically approximated as [31, 52]

$$\langle \mathcal{O}(t_0, x_i) \mathcal{O}(t_0, x'_i) \rangle \approx e^{-\Delta L}, \quad (15)$$

if the conformal dimension Δ of scalar operator \mathcal{O} is large enough, where L indicates the length of the bulk geodesic between the points (t_0, x_i) and (t_0, x'_i) on the AdS boundary. Usually the geodesic length above is divergent due to the contribution of the AdS boundary, one should eliminate the divergent part and use the renormalized geodesic length, defined by $\delta L =$

$L + 2 \ln z_0$ [30, 31], where z_0 is a UV cut-off that can be read from the boundary conditions

$$z(\frac{l}{2}) = z_0, v(\frac{l}{2}) = t_0, \quad (16)$$

in which l is the boundary separation between the points lies entirely over the x_1 direction and t_0 is the time of the thermalization probe moving from the shell to the boundary, which will be called as thermalization time later. Next we would like to rename x_1 as x and employ it to parameterize the trajectory such that the proper length is given by

$$L = 2 \int_0^{\frac{l}{2}} dx \frac{\sqrt{\Pi}}{z}, \quad (17)$$

with

$$\Pi = 1 - 2z'(x)v'(x) - H(v, z)v'(x)^2, \quad (18)$$

To minimize the length of the geodesic, we need to solve the two equations of motion for $z(x)$ and $v(x)$ respectively. Varying the length functional in Eq.(17), we get

$$\begin{aligned} z(x)\sqrt{\Pi}\partial_x\left(\frac{z'(x) + H(v, z)v'(x)}{z(x)\sqrt{\Pi}}\right) &= \frac{1}{2} \frac{\partial H(v, z)}{\partial v(x)} v'^2(x), \\ z(x)\sqrt{\Pi}\partial_x\left(\frac{v'(x)}{z(x)\sqrt{\Pi}}\right) &= \frac{1}{2} \frac{\partial H(v, z)}{\partial z(x)} v'^2(x) + \frac{\Pi}{z(x)}. \end{aligned} \quad (19)$$

To solve these equations, we need to consider the symmetry of the geodesic and impose the following initial conditions

$$z(0) = z_*, v(0) = v_*, v'(0) = z'(0) = 0. \quad (20)$$

Next we intend to solve the equations of motion in Eq.(19) numerically with the help of the initial conditions in Eq.(20). During the numerics, we will set the shell thickness $v_0 = 0.01$ and UV cut-off $z_0 = 0.01$ respectively. In addition, the mass M will be set to $\frac{1}{2}$ as done in [12]. In this case, with Eq.(9), we can check whether there is a horizon for different noncommutative parameter θ , which is plotted in Figure (1). From Figure (1), we know that for $\theta < 0.1234$, there is always a horizon while for $\theta > 0.1234$, there is not a horizon. That is, for $\theta < 0.1234$ a static black hole will be formed at the last stage of the gravitational collapse process, which indicates that the non-equilibrium state will approach to an equilibrium state lastly from the viewpoint of duality. For $\theta > 0.1234$, though a black brane will not be formed, we will also use the renormalized geodesic length to probe the

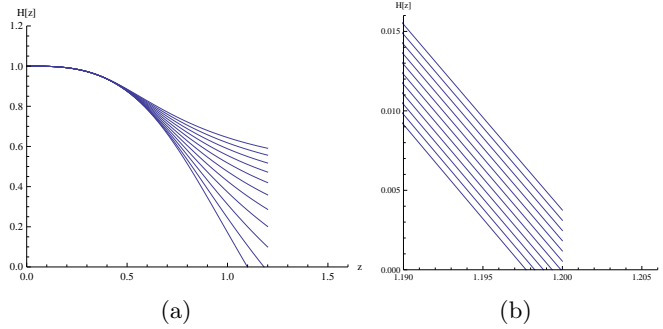


Figure 1: In (a), θ changes from 0.1 to 0.3 with step $\theta = 0.02$, in (b), θ changes from 0.123 to 0.124 with step $\theta = 0.0001$.

collapse of the shell so that we can know whether it will collapse all the time. The time for the shell collapse from the pure AdS to the stable state is also called thermalization time though we can not define an equilibrium state strictly in this case.

Firstly, we will set different initial time to explore whether the effect of the noncommutative parameters is the same at different stage. In Table (1), we list the thermalization time for different noncommutative parameters at different initial time v_* . From it, we know that for a fixed initial time, as the noncommutative parameters raise, the thermalization time increases firstly and then decreases step by step. Especially, for the large initial time, $v_* = -0.111$, the thermalization time decreases in advance. So we can conclude that the thermalization time for different noncommutative parameters is non-monotonic. In addition, at $v_* = -0.111$, we also plot the motion profiles of the geodesic for different noncommutative parameters, which are shown in Figure (2). In (a) and (b) in Figure (2), we know that the spacetimes own horizons, thus we can distinguish whether a static black brane have been formed by checking whether the shell has been dropped into the horizon. It is obvious that the shell in (a) has been dropped into the horizon while the shell in (b) is out of the horizon. A static black brane thus has been formed in (a) while the shell is collapsing in (b), which implies that the quark gluon plasma in the dual conformal theory has been thermalized for the case $\theta = 0.01$ while it is thermalizing for the case $\theta = 0.1$. In other words, as the noncommutative parameter increases, the thermalization will be delayed. In (c) and (d) in Figure (2), because there is not a horizon, we only know that the shell is collapsing, which implies that the quark gluon plasma in the dual conformal theory is thermalizing.

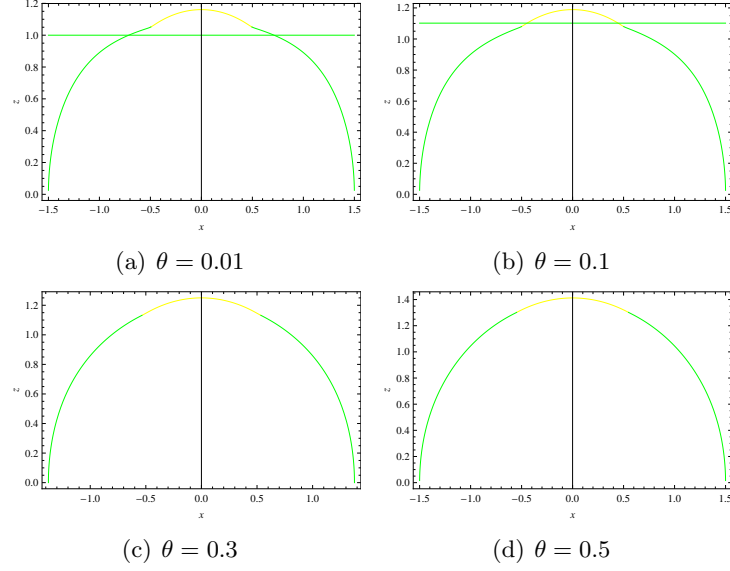


Figure 2: Motion profile of the geodesic in the noncommutative Vaidya AdS black brane with the same boundary separation and initial time. The black brane horizon is indicated by the horizontal green line. The position of the shell is described by the junction between the yellow line and green line.

	$\theta = 0.01$	$\theta = 0.1$	$\theta = 0.3$	$\theta = 0.5$	$\theta = 0.7$
$v_* = -0.888$	0.597428	0.597526	0.601945	0.605219	0.606315
$v_* = -0.444$	0.995173	1.02105	1.07147	1.0729	1.06914
$v_* = -0.111$	1.27647	1.33883	1.43042	1.42512	1.41624

Table 1: The thermalization time t_0 of the geodesic probe for different noncommutative parameters θ and different initial time v_* with the same boundary separation $l = 3$.

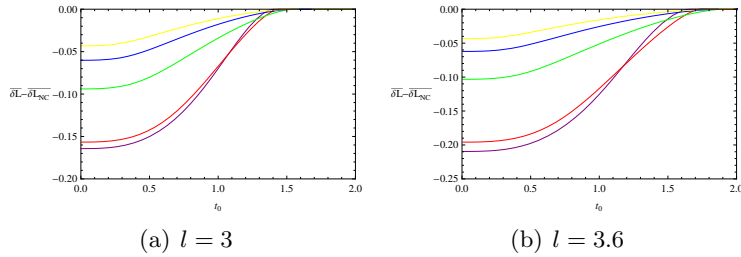


Figure 3: Thermalization of the renormalized geodesic lengths for different θ at a fixed boundary separation. The yellow line, blue line, green line, red line and purple line correspond to $\theta = 0.7, 0.5, 0.3, 0.1, 0.01$ respectively.

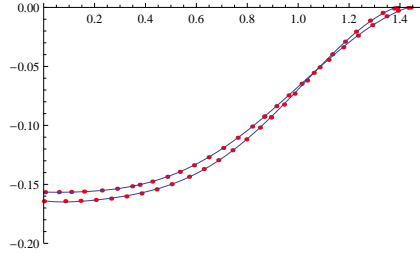


Figure 4: Comparison of the function in Eq.(3.10) with the numerical result for the case $\theta = 0.01, 0.1$ at the boundary separation $l = 3$.

With the numerical result of $z(x)$, we can study the renormalized geodesic length. As done in [30, 31, 32], we are interested in the l independent quantity $\overline{\delta L} - \overline{\delta L_{NC}}$ with $\overline{\delta L_{NC}} \equiv \delta L_{NC}/l$ being the length of the late stage. Figure (3) gives the relation between the renormalized geodesic length and thermalization time for different noncommutative parameters θ at a fixed boundary separation. From Figure (3), we know that for large noncommutative parameters, $\theta = 0.3, 0.5, 0.7$, though the background spacetimes have not horizons, the shell will not collapse all the time. At the last stage, they will stop in a stable state at the same thermalization time. But for different θ , the thermalization velocity is different, which can be read off from the slope of the thermalization curve. It should be noted that the thermalization time for the background spacetime without a horizon, $\theta = 0.3, 0.5, 0.7$, is longer than that with a horizon, $\theta = 0.01, 0.1$. That is, as a static black brane is formed the shell for large θ is still collapsing. In the small θ region, we can observe that the thermalization time increases as θ raises. As the boundary separation raises, this effect is more obvious, please see (a) and (b) in Figure (3). Therefore we know that as the noncommutative parameter increases, the thermalization will be delayed. This phenomenon has been also observed previously when we study the motion profile of the geodesic. In addition, in Figure (3), we find for a fixed boundary separation there is always a time range in which the renormalized geodesic length for different θ takes the same value nearly. That is, during that time range, the noncommutative parameters have few effect on the renormalized geodesic length. In [35, 36], effect of the Gauss-Bonnet coefficient on the thermalization time was investigated, they also found this phenomenon.

Interestingly, we find the thermalization curve for a fixed noncommutative parameter in Figure (3) can be fitted as a function of t_0 . Here we take the case $\theta = 0.01, 0.1$ as examples. At the boundary separation $l = 3$, the

numeric curves for $\theta = 0.01, 0.1$ can be fitted as

$$\begin{cases} g_{0.01} = -0.163841 - 0.0300155t_0 + 0.260142t_0^2 - 0.685112t_0^3 \\ \quad + 1.10426t_0^4 - 0.703409t_0^5 + 0.148517t_0^6 \\ g_{0.1} = -0.156499 - 0.00586248t_0 + 0.0557009t_0^2 - 0.0778527t_0^3 \\ \quad + 0.32609t_0^4 - 0.272237t_0^5 + 0.0634748t_0^6 \end{cases} \quad (21)$$

Figure (4) is the comparison result of the numerical curves and fitting function curves. It is obvious that at the order of t_0^6 , the thermalization curve can be described well by the fitting function⁵. With this function, we can get the thermalization velocity, defined by $v_-T \equiv d(\delta\bar{L} - \delta\bar{L}_{NC})/dt$, and thermalization acceleration, defined by $a_-T \equiv d^2(\delta\bar{L} - \delta\bar{L}_{NC})/dt^2$, which are plotted in Figure (5). From the velocity curve, we can observe that there is a phase transition point at the middle stage of the thermalization, which divides the thermalization into an accelerating and a decelerating phase. The phase transition points for different noncommutative parameters can be read off from the null point of the acceleration curve. It is easy to find that in the time range, $0 < t_0 < 1.024$ for $\theta = 0.01$ and $0 < t_0 < 1.0125$ for $\theta = 0.1$, the thermalization is an accelerating process while for the other time range, it is a decelerating process before it approaches to the equilibrium state. Obviously, as the noncommutative parameter increases, the value of the phase transition point decreases. That is, larger the noncommutative parameter is, earlier the thermalization decelerates. This result also indicates that the large noncommutative parameter delays the thermalization.

From the acceleration curve, we find that during the acceleration phase, the acceleration is not enhanced always, which first decreases, then increases, and decreases once again. In other words, the acceleration undergoes two phase transition during the thermalization.

4. Conclusions

Gravitational collapse of a thin shell in the noncommutative geometry is probed by the renormalized geodesic length, which is dual to probe the thermalization in conformal field theory by the two-point functions. We first study the motion profiles of the geodesic, and then the renormalized geodesic length. For the spacetime without a horizon, we find the shell will

⁵For higher order power of t_0 , we find it has few contributions to the thermalization, including the phase transition point which will be discussed next.

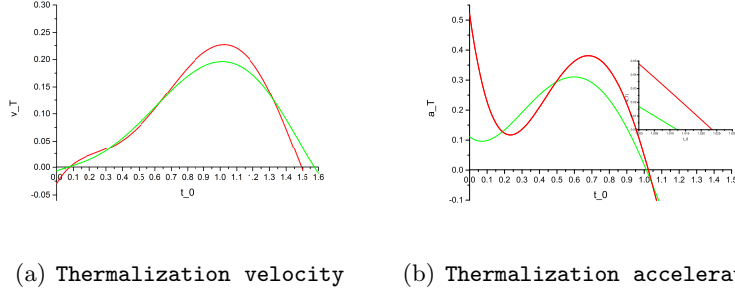


Figure 5: Thermalization velocity and acceleration of the renormalized geodesic in a noncommutative Vaidya AdS black brane. The red line and green line correspond to $\theta = 0.01$ and $\theta = 0.1$.

not collapse all the time but will stop in a stable state at the same thermalization time. For the spacetime with a horizon, we investigate how the noncommutative parameter affects the thermalization process by numerical calculation and fitting function. From the numerical results, we know that the noncommutative parameter delays the thermalization process. In [32, 33, 34, 36], effect of the charge on the thermalization time is investigated. They found that as the charge increases, the thermalization time decreases. Obviously, the noncommutative parameter has the similar effect on the thermalization time as the charge⁶. In addition, for both the thermalization probes, we observe an overlapped region where the noncommutative parameter has few influence on them for a fixed boundary separation. In fact, this phenomenon has also been observed in modified gravity[35, 36]. It is explained that this effect arises from the difference of the temperature of the dual conformal field for the thermalization only becomes fully apparent at distances of the order of the thermal screening length $\tilde{l}_D \sim (\pi T)^{-1}$, where T is the temperature of the dual conformal field.

We also find the fitting functions of the thermalization curves. With it, we get some useful information about the thermalization. We first get the thermalization velocity at a fixed noncommutative parameter. From the velocity curve, we know that the thermalization is non-monotonic, which is indicated by the negative value of the thermalization velocity at the initial thermalization time. Secondly we find there is a phase transition point

⁶In this case, how to distinguish the effect of charge and noncommutative parameters on the thermalization time becomes necessary and important, we will address this problem later.

during the thermalization, which divides the thermalization into an acceleration phase and a deceleration phase. The phase transition point is found to be decreased as the noncommutative parameter increases. We also obtain the thermalization acceleration, which is found to be not enhanced always during the acceleration phase. Recently Liu et al. [53, 54], followed by [55], have investigated the nonlocal observables analytically. They found that the thermalization can be divided into four regimes: pre-local-equilibration quadratic growth regime, post-local-equilibration linear growth regime, a late-time regime, and a saturation regime. In each regime, they obtained the analytical functions of the nonlocal observables, which are shown to be the linear function of the thermalization time. Obviously, our result agrees with their result in part for we also obtain this linear relation.

Acknowledgements

We are grateful to Hongbao Zhang for his various valuable suggestions about this work. This work is supported by the National Natural Science Foundation of China (Grant Nos. 11405016, 11365008, 61364030) and the natural science foundation of Hubei Province (No. 2014CFB608). .

References

References

- [1] H. S. Snyder, Phys. Rev. 71 (1947) 38.
- [2] N. Seiberg and E. Witten, J. High Energy Phys. 09032, (1999)
- [3] A. Hashimoto and N. Itzhaki, Phys. Lett. B 465, 142 (1999); M. Al-
ishahiha, Y. Oz, M. M. Sheikh-Jabbari, JHEP 9911, 007 (1999).
- [4] J. M. Maldacena and J. G. Russo, JHEP 9909, 025 (1999).
- [5] A. Smailagic and E. Spallucci, J. Phys. A 36, L467 (2003)
- [6] A. Smailagic and E. Spallucci, J. Phys. A 36, L517 (2003),
- [7] P. Nicolini, A. Smailagic and E. Spallucci, Phys. Lett. B 632, 547 (2006).
- [8] W. Kim, E. J. Son and M. Yoon, JHEP 0804, 042 (2008); B. Vakili, N.
Khosravi and H. R. Sepangi, Int. J. Mod. Phys. D 18, 159 (2009); W. H.
Huang and K. W. Huang, Phys. Lett. B 670, 416 (2009); Y. S. Myung,
Y. W. Kim and Y. J. Park, JHEP 0702, 012 (2007); R. Banerjee, B. R.
Majhi, S. Samanta, Phys. Rev. D 77, 124035 (2008).

- [9] Y.-G. Miao, Z. Xue and S.-J. Zhang, J. Mod. Phys. D 21, 1250018 (2012); Y.-G. Miao, Z. Xue, and S.-J. Zhang, Gen. Relativ. Gravit. 44, 555,(2012); S. W. Wei, Y. X. Liu, Z. H. Zhao and C.-E Fu, Area spectrum of Schwarzschild black hole inspired by noncommutative geometry, arXiv:1004.2005[hep-th].
- [10] K. Nozari and S. H. Mehdipour, Class. Quant. Grav. 25, 175015, (2008); K. Nozari and S. H. Mehdipour, JHEP 0903, 061 (2009); S. H. Mehdipour, Phys. Rev. D 81, 124049 (2010).
- [11] S. Ansoldi, P. Nicolini, A. Smailagic and E. Spallucci, Phys. Lett. B 645, 261 (2007); P. Nicolini and E. Spallucci, Class. Quant. Grav. 27, 015010 (2010); L. Modesto and P. Nicolini, Phys. Rev. D 82, 104035 (2010); E. Spallucci, A. Smailagic and P. Nicolini, Phys. Lett. B 670, 449 (2009); M. Park, Phys. Rev. D 80, 084026, (2009).
- [12] C. Ding, J. Jing, JHEP 10, 052 (2011); C. Ding *et al.*, Phys. Rev. D 83, 084005 (2011).
- [13] P. Nicolini, Giorgio Torrieri, JHEP 1108, 097 (2011).
- [14] W. Fischler, A. Kundu, S. Kundu, JHEP 01, 137 (2014).
- [15] S. Pramanik, S. Das, S. Ghosh, Noncommutative Extension of AdS/CFT and Holographic Superconductors, arXiv:1401.7832 [hep-th].
- [16] R. B. Mann, P. Nicolini, Phys. Rev. D 84, 064014 (2011).
- [17] M. Gyulassy and L. McLerran, Nucl. Phys. A 750, 30 (2005)
- [18] U. H. Danielsson, E. Keski-Vakkuri and M. Kruczenski, Nucl. Phys. B 563, 279 (1999).
- [19] D. Garfinkle and L. A. Pando Zayas, Phys. Rev. D 84, 066006 (2011).
- [20] D. Garfinkle, L. A. Pando Zayas and D. Reichmann, JHEP 1202, 119 (2012).
- [21] A. Allais and E. Tonni, JHEP 1201 102 (2012).
- [22] S. R. Das, J. Phys. Conf. Ser. 343, 012027 (2012).
- [23] D. Steineder, S. A. Stricker and A. Vuorinen, probing the pattern of holographic thermalization with photons, arXiv:1304.3404 [hep-ph].

- [24] B. Wu, JHEP 1210, 133 (2012).
- [25] X. Gao, A. M. Garcia-Garcia, H. B. Zeng, H. Q. Zhang, Lack of thermalization in holographic superconductivity, arXiv:1212.1049 [hep-th].
- [26] A. Buchel, L. Lehner, R. C. Myers and A. van Niekerk, JHEP 1305, 067 (2013).
- [27] V. Keranen, E. Keski-Vakkuri, L. Thorlacius, Phys. Rev. D 85, 026005 (2012).
- [28] B. Craps *et al.*, Gravitational infall in the hard wall model, arXiv:1406.1454[hep-th].
- [29] B. Craps *et al.*, JHEP 1402, 120 (2014).
- [30] V. Balasubramanian *et al.*, Phys. Rev. Lett. 106, 191601 (2011).
- [31] V. Balasubramanian *et al.*, Phys. Rev. D 84, 026010 (2011).
- [32] D. Galante and M. Schvellinger, JHEP 1207, 096 (2012).
- [33] E. Caceres and A. Kundu, JHEP 1209, 055 (2012).
- [34] E. Caceres, A. Kundu, D. L. Yang, Jet Quenching and Holographic Thermalization with a Chemical Potential, arXiv:1212.5728 [hep-th].
- [35] X. X. Zeng and W. Liu, Phys. Lett. B 726, 481 (2013).
- [36] X. X. Zeng, X. M. Liu, and W. Liu, JHEP 03, 031 (2014)
- [37] W. H. Baron and M. Schvellinger, Quantum corrections to dynamical holographic thermalization: entanglement entropy and other non-local observables, arXiv:1305.2237 [hep-th].
- [38] Y. Z. Li, S. F. Wu, G. H. Yang, Phys. Rev. D 88, 086006 (2013).
- [39] W. Baron, Damian Galante and M. Schvellinger, JHEP 1303, 070 (2013).
- [40] I. Arefeva, A. Bagrov, A. S. Koshelev, JHEP 07, 170 (2013).
- [41] V. E. Hubeny, M. Rangamani, E. Tonni, JHEP 05, 136 (2013).
- [42] I. Y. Arefeva, I. V. Volovich, On Holographic Thermalization and De-thermalization of Quark-Gluon Plasma, arXiv:1211.6041 [hep-th].

- [43] V. Balasubramanian *et al.*, JHEP 04, 069 (2013).
- [44] V. Balasubramanian *et al.*, JHEP 10, 082 (2013).
- [45] V. Balasubramanian *et al.*, Phys. Rev. Lett. 111, 231602 (2013).
- [46] V. Balasubramanian *et al.*, Holographic Thermalization, Phys. Rev. Lett. 113, 071601 (2014).
- [47] V. Cardoso *et al.*, Holographic thermalization, quasinormal modes and superradiance in Kerr-AdS, arXiv:1312.5323[hep-th].
- [48] V. E. Hubeny, H. Maxfield, Holographic probes of collapsing black holes, arXiv:1312.6887[hep-th].
- [49] W. Fischler, S. Kundu, J. F. Pedraza, JHEP 07, 021 (2014); J. F. Pedraza, Evolution of non-local observables in an expanding boost-invariant plasma, arXiv:1405.1724 [hep-th]; E. Caceres, A. Kundu, J. F. Pedraza, W. Tangarife, JHEP 01, 084 (2014); X. X. Zeng, D. Y. Chen, L. F. Li, Holographic thermalization and gravitational collapse in the spacetime dominated by quintessence dark energy, arXiv:1408.6632[hep-th]; M. Alishahiha, A. F. Astaneh, M. R. M. Mozaffar, Thermalization in backgrounds with hyperscaling violating factor, arXiv:1401.2807[hep-th]; M. Alishahiha, M. R. M. Mozaffar, M. R. Tanhayi, Evolution of Holographic n-partite Information, arXiv:1406.7677[hep-th].
- [50] A. Chamblin, R. Emparan, C. V. Johnson and R. C. Myers, Phys. Rev. D 60, 064018 (1999).
- [51] J. J. Oh and C. Park, JHEP 1003,086 (2010).
- [52] V. Balasubramanian and S. F. Ross, Phys. Rev. D 61, 044007 (2000).
- [53] H. Liu and S. J. Suh, Phys. Rev. Lett. 112, 011601 (2014).
- [54] H. Liu and S. J. Suh, Phys. Rev. D 89, 066012 (2014).
- [55] M. Alishahiha, A. F. Astaneh, M. R. M. Mozaffar, Thermalization in backgrounds with hyperscaling violating factor, arXiv:1401.2807[hep-th]; M. Alishahiha, M. R. M. Mozaffar, M. R. Tanhayi, Evolution of Holographic n-partite Information arXiv:1406.7677[hep-th]; P. Fonda, L. Franti, V. Keranen, E. Keski-Vakkuri, L. Thorlacius and E. Tonni, JHEP 08, 051 (2014).

